The Stress-Relief Cracking Susceptibility of a New Ferritic Steel — Part 1: Single-Pass Heat-Affected Zone Simulations

The effects of energy input and postweld heat treatment temperature on the stress-relief cracking susceptibility of a new ferritic steel were investigated and compared to conventional 2.25Cr-1Mo steel

BY J. G. NAWROCKI, J. N. DUPONT, C. V. ROBINO AND A. R. MARDER

ABSTRACT. The stress-relief cracking (SRC) susceptibility of single-pass welds in a new ferritic steel, HCM2S, has been evaluated and compared to 2.25Cr-1Mo steel using Gleeble thermal simulation techniques. HCM2S was found to be more susceptible to stress-relief cracking than 2.25Cr-1Mo steel. Simulated coarse-grained heat-affected zones (CGHAZ) were produced that correspond to the thermal cycles expected when depositing single-pass welds using a range of energy inputs and tested at various simulated postweld heat treatment (PWHT) temperatures. Both alloys were tested at a stress of 325 MPa. The 2.25Cr-1Mo steel was also tested at 270 MPa to normalize for the difference in yield strength between the two materials. Light optical and scanning electron microscopy were used to characterize the simulated CGHAZ microstructures. The simulated as-welded CGHAZ of each alloy consisted of lath martensite or bainite and had approximately equal prior austenite grain sizes. The as-welded hardness of the simulated 2.25Cr-1Mo steel CGHAZ was significantly higher than that of the HCM2S alloy. Over the range studied, energy input had little effect on the as-welded microstructure or hardness of either alloy. The energy input also had no effect on the stress-relief cracking susceptibility of either material. Both alloys failed intergranularly along prior austenite grain boundaries under all test conditions. The 2.25Cr-1Mo steel samples experienced significant macroductility and some microductility when tested at 325 MPa. The ductility decreased significantly when tested at 270 MPa, but it was still higher than that of HCM2S at each test condition. The stress-relief cracking susceptibility was based on the ductility and resultant microstructures. Using these criteria, HCM2S is considered "extremely" to "highly susceptible" to stress-relief cracking at each energy input and postweld heat treatment, whereas 2.25Cr-1Mo steel would only be considered "slightly susceptible" tested at 325 MPa. The 2.25Cr-1Mo steel samples tested at 270 MPa are considered "slightly" to "highly susceptible" to stress-relief cracking at each PWHT temperature. The time to failure decreased with increasing PWHT temperature for each material. There was no significant difference in the times to failure between the two materials. Varying energy input and stress had no effect on the time to failure. The ductility, as measured by reduction in area, increased with increasing PWHT temperature for 2.25Cr-1Mo steel tested at both initial stress levels. However, PWHT temperature had no effect on the ductility of HCM2S. The hardness of the CGHAZ for 2.25Cr-1Mo steel decreased significantly after PWHT, but it remained constant for HCM2S. The differences in stress-relief cracking response are discussed in terms of the differences in composition and expected carbide precipitation sequence for each alloy during PWHT.

KEY WORDS

Stress-Relief Cracking
Ferritic Steel
Coarse-Grained HAZ
Alloy HCM2S
Thermal Cycles
Postweld Heat Treat
Chrome-Moly
Power Plant

J. G. NAWROCKI, J. N. DUPONT and A. R. MARDER are with the Department of Materials Science and Engineering, Lehigh University, Bethlehem, Pa. C. V. ROBINO is with Materials Joining Dept., Sandia National Laboratories, Albuquerque, N. Mex.

Introduction

2.25Cr-1Mo steel is commonly used for high-temperature applications in steam generators and pressure vessels for chemical and fossil power plants. Many components in these power plants operate at temperatures of approximately 300–600°C. New components fabricated from 2.25Cr-1Mo steel may require welding at both the fabrication and installation stages, and in-service material may be welded during repairs. In such applications, preheat and/or postweld heat treatment (PWHT) are often required to improve heat-affected zone (HAZ) mechanical properties and reduce susceptibility to hydrogen cracking. These preheat and PWHT steps represent a significant fraction of the overall fabrication/repair costs.

Recently, a new ferritic steel, denoted as HCM2S, was developed. HCM2S has been reported to exhibit improved mechanical properties and resistance to hydrogen cold cracking compared to conventional 2.25Cr-1Mo steel (Refs. 1–3). Table 1 compares the allowable composition ranges of both 2.25Cr-1Mo and the HCM2S alloy (Refs. 1, 4). The lowered carbon content improves weldability by reducing hardenability and the as-welded hardness of the HAZ. Although the carbon content of HCM2S and

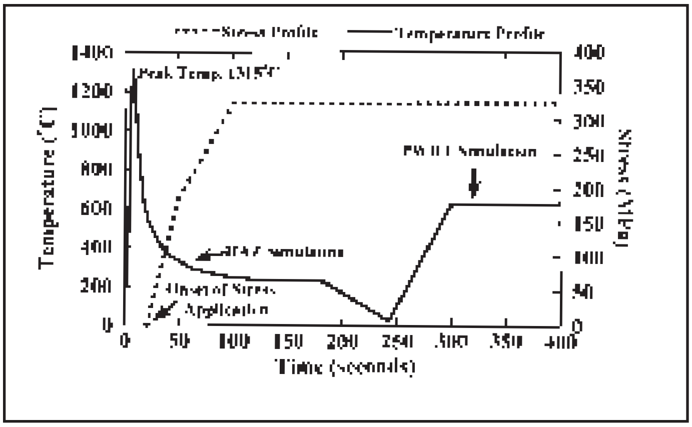

Fig. 1 — Schematic illustration of a stress-relief cracking test cycle.

Table 1 — Allowable Composition Range of HCM2S and 2.25Cr-1Mo Steel (wt-%)

Element	HCM2S (Ref. 1)	2.25Cr-1Mo (Ref. 5)
C	0.04–0.10	0.15
Cr	1.90–2.60	2.00–2.50
Mo	0.30	0.90–1.10
W	1.45–1.75	—
V	0.20–0.30	—
Nb	0.02–0.08	—
B	0.006	—
Al	0.03	—
Si	0.50	0.20–0.50
Mn	0.30–0.60	0.30–0.60
P	0.030	0.035
S	0.010	0.035

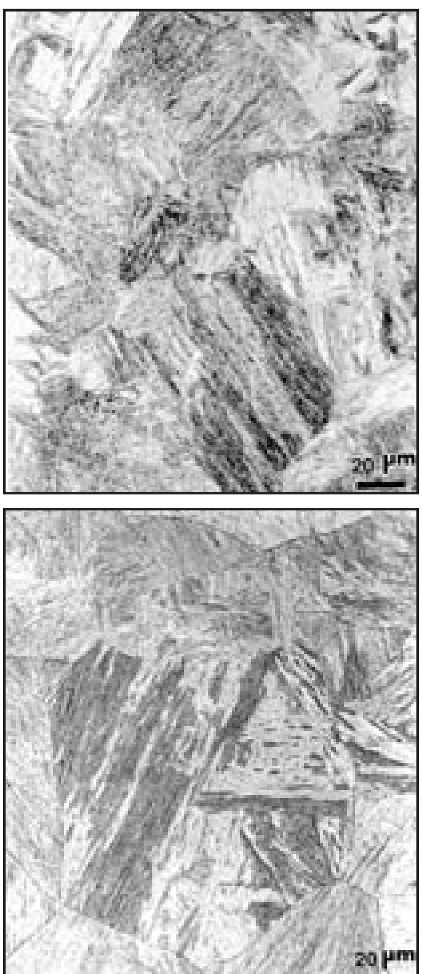

Fig. 2 — Representative coarse-grained heat-affected zone microstructure in the as-welded condition. A — 2.25 Cr-1Mo; B — HCM2S.

2.25Cr-1Mo can be identical, HCM2S is typically produced with a carbon content of ~0.06 wt-%, which is much lower than the typical carbon content of 2.25Cr-1Mo steel (Refs. 1–3, 5). In addition, the maximum allowable C content is 0.1 and 0.15 wt-% for HCM2S and 2.25Cr-1Mo steel, respectively. The creep rupture strength is improved by the substitution of Mo with W that acts as a solid-solution strengthening element. Vanadium and niobium are added to improve creep strength by way of carbide precipitation strengthening. Boron is also added to improve creep strength. It has recently been suggested that the improved weldability from these composition modifications may permit elimination of costly preheat and/or PWHT requirements. Although HCM2S has been shown to exhibit excellent mechanical properties and resistance to hydrogen cracking, the stress-relief cracking susceptibility had yet to be investigated.

Many low-alloy, creep-resistant steels such as 2.25Cr-1Mo steel are known to be susceptible to stress-relief cracking (Ref. 6). Stress-relief cracking is defined as intergranular cracking in the heat-affected zone or weld metal that occurs during exposure of welded assemblies to postweld heat treatments or high-temperature service (Ref. 7). Stress-relief cracking occurs primarily in the CGHAZ of a weldment. The general mechanism of stress-relief cracking is well documented in the literature and has been explained for low-alloy steels (Refs. 6–10). During typical fusion welding processes, the unmelted base material surrounding the weld pool is heated to a temperature very high in the austenite phase field. During this time, pre-existing carbides either dissolve or coarsen and austenite grain growth occurs. Due to the fast cooling rates during fusion welding, supersaturation of microalloying elements occurs as the austenite transforms to martensite (provided the alloy has sufficient hardenability). When the newly formed CGHAZ is exposed to elevated temperatures, alloy carbides (*e.g.* VC, NbC) preferentially precipitate at dislocations in the prior austenite grain interiors, thereby causing considerable strengthening. These carbides retard dislocation movement and do not allow residual stresses to relax through plastic deformation of the grains. The microstructure may also contain precipitate-free denuded zones adjacent to prior austenite grain boundaries. These denuded zones may be due to grain boundary carbides that have depleted the adjacent matrix of carbon and alloying elements (Refs. 11, 12) or the formation of a second phase during cooling after welding (Ref. 13). Along with this, classical temper embrittlement can occur, which is the segregation of tramp elements to prior austenite grain boundaries during cooling or elevated temperature exposure. These segregants lower the cohesive strength of the boundaries and, together with the presence of a denuded zone, can lead to brittle intergranular failure.

Previous work has been conducted to understand the stress-relief cracking susceptibility of 2.25Cr-1Mo steel. However, the stress-relief cracking response of this HCM2S alloy is currently unknown. Therefore, the objective of this work is to evaluate the stress-relief cracking susceptibility of HCM2S relative to 2.25Cr-1Mo steel expected in single pass welds deposited with a range of heat inputs and several PWHT temperatures. The results may be useful for determining the conditions under which HCM2S may be used in the pressure vessel and utility industries.

Experimental Procedure

Stress-Relief Cracking Tests

The alloy compositions of the 2.25Cr-1Mo and HCM2S steels used in this research are summarized in Table 2. Stress-relief cracking tests were performed using a Gleeble 1000 thermomechanical simulator. Unnotched, cylindrical test samples (105 mm long and 10 mm diameter) with threaded ends were used. A schematic illustration of the stress-relief cracking thermomechanical test cycle can be seen in Fig. 1. Samples were subjected to single-pass weld thermal simulation cycles representative of 2, 3 and 4 kJ/mm energy inputs with a peak temperature of 1315°C and a preheat temperature of 93°C. The thermal cycles are based on actual data from SMA welds on carbon steel (Refs. 14, 15). A tensile stress was imposed on the sample during cooling and held for the duration of the test to simulate the residual stresses present in an actual weldment. After cooling to room temperature, the sample was then subjected to a simulated programmed postweld heat treatment temperature and held at constant temperature and load (that corresponds to the initial stress level) until failure. The load is actually constant and not the stress because the stress will change as the cross-sectional area of the specimen changes. Therefore, when the stress level is mentioned hereafter, it corresponds to the initial stress level. The simulated postweld heat treatment temperatures ranged from 575–725°C. Both materials were tested at a stress of 325 MPa and the 2.25Cr-1Mo steel was also tested at a stress of 270 MPa. The initial stress levels (325 MPa for HCM2S and 270 MPa for 2.25Cr-1Mo) were chosen based on the yield strength of the alloys at ~650°C. The yield strengths of the CGHAZ of these alloys at the test temperatures used in this research are unavailable and therefore the above values were chosen because 650°C is near the middle of the test temperature range. The 2.25Cr-1Mo steel samples tested at 270 MPa were produced using an energy input of 2 kJ/mm. The maximum residual stress present in a weldment is typically at or near the yield strength (Ref. 16). Therefore, the lower stress was used because the yield strength of HCM2S is typically higher than that of 2.25Cr-1Mo steel and lowering the stress serves to help normalize the yield strength differences between the two materials. A constant load test is more severe than a constant displacement or stress relaxation test because the load is not allowed to relax and the sample is often taken to failure. However, the mechanism of stress-relief cracking was effectively simulated and the constant load test is relatively easy to perform. These tests were performed under a vacuum of approximately 100 millitorr to prevent decarburization and oxidation of the samples as well as decoherence of the thermocouples. The time to failure was taken to be the time when the PWHT temperature was reached to the time of rupture. The ductility was determined as the reduction in area during PWHT.

One half of each fractured sample was reserved for fractographic examination by scanning electron microscopy (SEM). The remaining half was electroless Ni-coated to provide edge retention of the fracture surface. Longitudinal cross-sectional samples were then polished to a 0.04 µm finish using colloidal silica. Microhardness traverses were performed on samples in the as-welded condition and after SRC testing using a Knoop indenter and a 500-g load. Samples were etched using either 2% Nital or Vilella's reagent and observed using light optical microscopy (LOM). Prior austenite grain size measurements were made in accordance with ASTM E112-84.

Table 2 — Chemical Composition of HCM2S and 2.25Cr-1Mo Steels (wt-%)

Element	HCM2S (Ref. 1)	2.25Cr-1Mo (Ref. 5)
C	0.06	0.13
Si	0.25	0.2
Mn	0.48	0.5
P	0.013	0.008
S	0.006	0.001
Cr	2.4	2.3
Mo	0.09	1.04
W	1.5	NM
V	0.24	0.004
Nb	0.050	0.001
B	0.0036	NM
Al	0.013	NM
Sn	0.01	0.01
Sb	0.01	<0.001
As	0.01	0.006
Fe	balance	balance

NM: not measured

Results

Stress-Relief Cracking Tests

Typical as-welded CGHAZ microstructures of each alloy are shown in Fig. 2. Each thermal cycle produced a microstructure consisting of lath martensite and/or bainite with similar prior austenite grain sizes (~50 µm). Hardness tra-

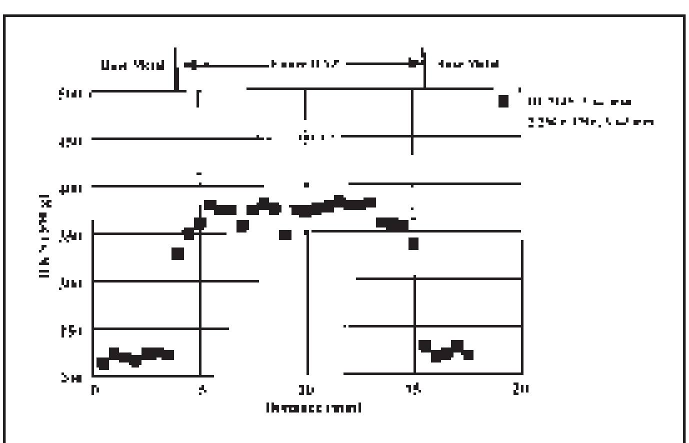

Fig. 3 — Microhardness traverse across simulated heat-affected zones. The traverse was across the sample between the jaws of the Gleeble.

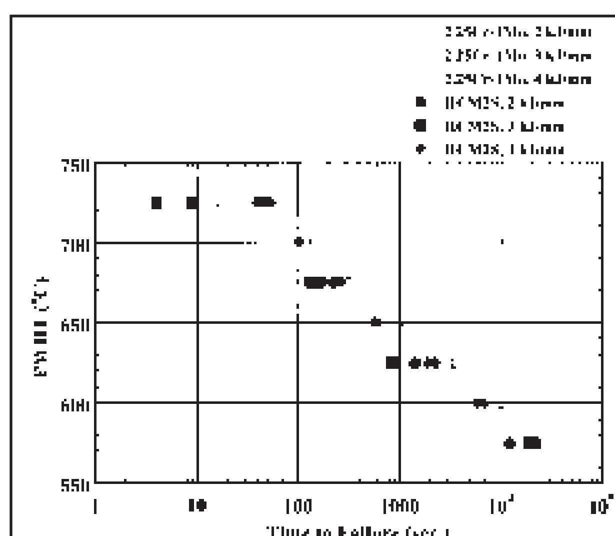

Fig. 4 — Postweld heat treatment temperature vs. time to failure at various energy inputs.

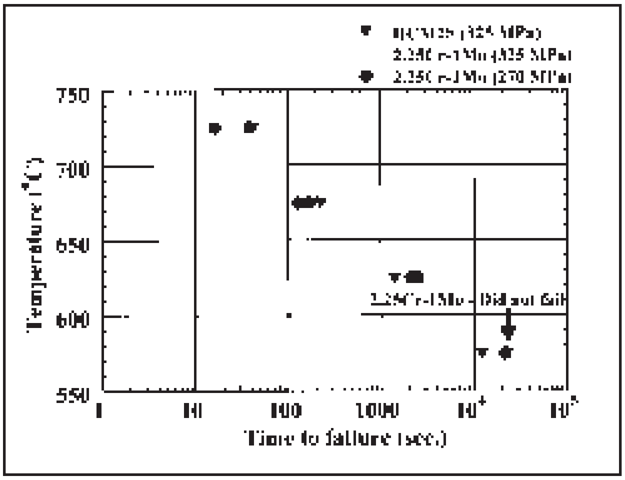

Fig. 5 — Postweld heat treatment temperature vs. time to failure for an energy input of 2 kJ/mm along with lowered stress values for 2.25Cr-1Mo steel.

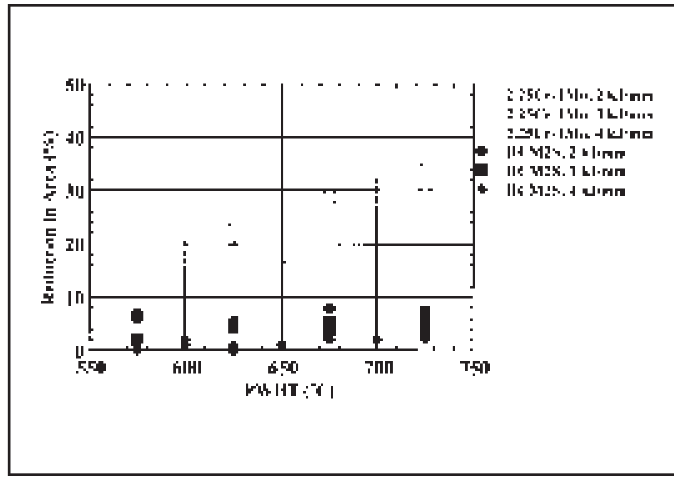

Fig. 6 — Reduction in area as a function of PWHT temperature at various energy inputs.

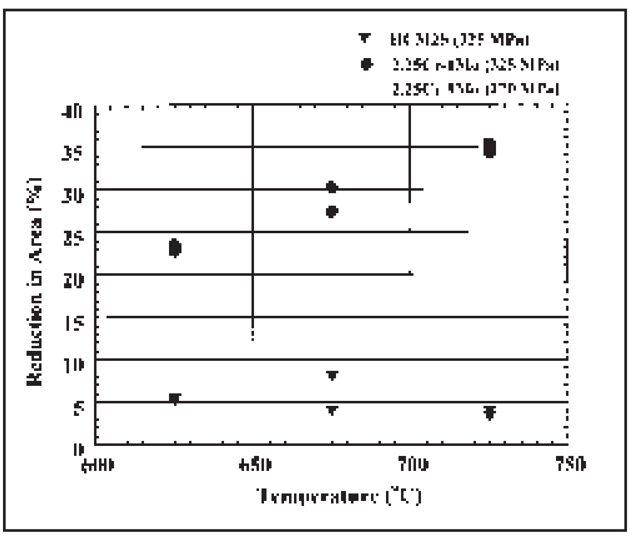

Fig. 7 — Reduction in area as a function of PWHT temperature for an energy input of 2 kJ/mm along with lowered stress values for 2.25Cr-1Mo steel.

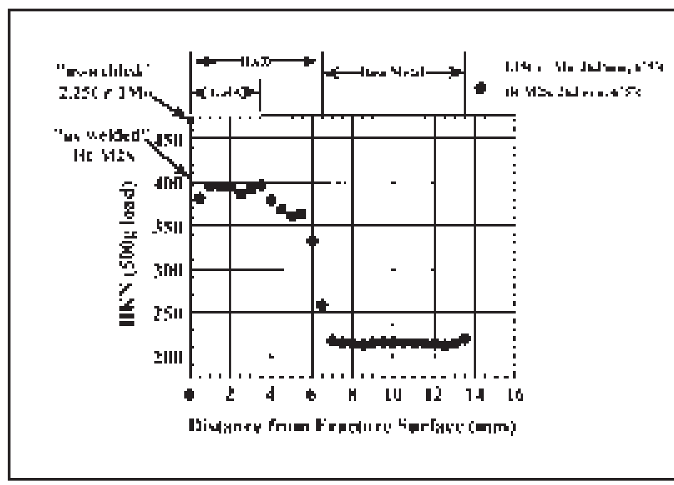

Fig. 8 — Microhardness traces acquired from HAZ samples (2 kJ/mm) after failure during a PWHT of 675°C.

verses from each alloy in the as welded condition (energy input of 3 kJ/mm) are presented in Fig. 3. These traverses are across the entire region between the jaws of the Gleeble and represent the entire HAZ along with unaffected base material. Although the base metal hardness of each alloy is similar (~225 HKN), the 2.25Cr-1Mo steel has a much higher peak hardness in the CGHAZ (~470 HKN) than HCM2S (~375 HKN) due to the higher C content. The CGHAZ extends from approximately 6.5 mm to 13.5 mm in Fig. 3. The hardness of the simulated CGHAZ of HCM2S corresponds well with hardness values of actual welds taken for comparison (~370 HKN). The microstructure of the CGHAZ is more likely to be martensite than bainite due to the large effect of carbon content on the as-welded hardness of the CGHAZ. Figure 4 shows the postweld heat treatment temperature vs. time to failure for both alloys tested under an initial stress of 325 MPa and various energy inputs and postweld heat treatments. It is important to note every failure occurred in the CGHAZ. In general, as the PWHT temperature increased, the time to failure decreased for both materials. There is no discernable difference between the two materials, and the change in energy input is shown to have very little effect. Varying energy input also had no discernable effect on the CGHAZ peak hardness, implying the cooling rate (for 100% martensite formation) in these simulations was faster than the critical cooling rate for these materials. Figure 5 compares the time to failure for both alloys tested at an energy input of 2 kJ/mm and an initial stress of 325 MPa as well as 2.25Cr-1Mo steel tested at an initial stress of 270 MPa. It can be seen the change in stress had no effect on the time to failure for the 2.25Cr-1Mo alloy. The 2.25Cr-1Mo samples tested at 575°C (325 and 270 MPa) did not fail after six hours and the tests were stopped. Figure 6 shows the variation in reduction in area as a function of postweld heat treatment temperature at various energy inputs for each alloy tested at 325 MPa. For 2.25Cr-1Mo, the ductility increased considerably with in-

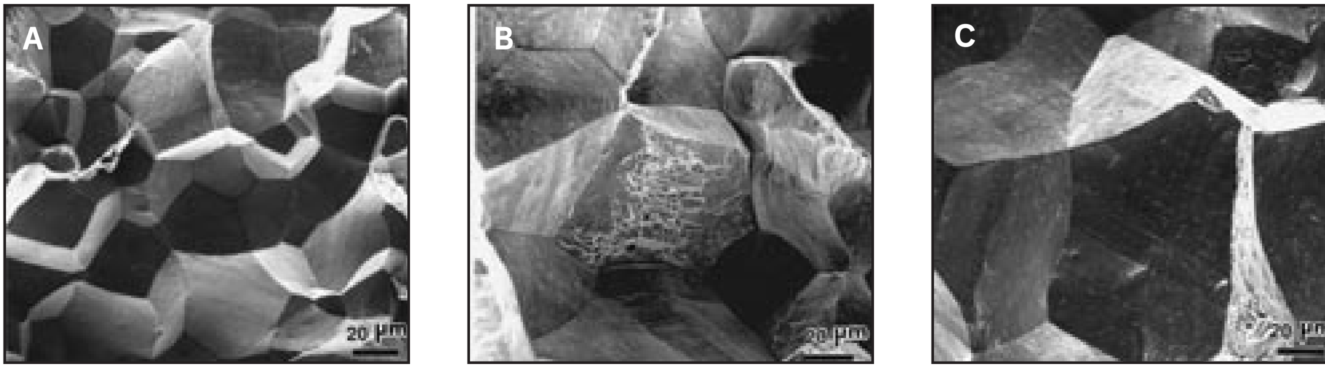

Fig. 9 — Scanning electron microscopy photomicrographs of fracture surfaces. Samples produced using an energy input of 2 kJ/mm and tested at a PWHT temperature of 675°C. A — HCM2S; B — 2.25Cr-1Mo tested at 325 MPa; C — 2.25Cr-1Mo tested at 270 MPa.

creasing PWHT temperature. In contrast, HCM2S shows no clear variation in ductility with PWHT temperature. Again, there is no clear correlation between the ductility and the energy input for a given PWHT. Figure 7 shows the variation in reduction in area as a function of PWHT for both alloys tested at an energy input of 2 kJ/mm and a stress of 325 MPa as well as 2.25Cr-1Mo steel tested at 270 MPa. The reduction in area at 270 MPa is much lower than the reduction in area at 325 MPa at each PWHT temperature for the 2.25Cr-1Mo steel. Figure 8 compares typical hardness traverses acquired from each material after being subjected to an energy input of 2 kJ/mm, a PWHT of 675°C and a stress of 325 MPa. The original CGHAZ extends approximately 3.5 mm from the fracture surface. The hardness of the HCM2S is constant across the CGHAZ, but the hardness increases near the end of the CGHAZ in 2.25Cr-1Mo steel. It is unclear as to why this occurs, but it may be due to the increased elongation of the 2.25Cr-1Mo samples. Necking during the test may cause a temperature gradient to form, thereby causing the variation in hardness with distance. The peak hardness of the CGHAZ in the 2.25Cr-1Mo steel was considerably higher than HCM2S in the as-welded condition. However, the hardness of the 2.25 Cr-1Mo steel decreased considerably after PWHT (from 470 HKN to ~325 HKN), while the HCM2S hardness exhibits no detectable change although the times to failure (time of exposure to PWHT) were equivalent. This behavior was typical of each sample tested at 325 MPa.

The HCM2S alloy generally showed more evidence of brittle intergranular failure. Figure 9 shows SEM photomicrographs of samples produced using a thermal cycle representative of an energy input of 2 kJ/mm and tested at 675°C. The samples represented in Fig. 9A (HCM2S) and 9B (2.25Cr-1Mo) were tested at a stress of 325 MPa and the sample shown in Fig. 9C was tested at 270 MPa (2.25Cr-1Mo). Each of the samples failed intergranularly along prior austenite grain boundaries. These microstructural features indicate the test conditions properly simulate the stress-relief cracking mechanism. In comparing the two samples tested at 325 MPa, the 2.25Cr-1Mo steel exhibits some microductility on grain surfaces (Fig. 9B), whereas the HCM2S sample has primarily smooth, featureless grain surfaces — Fig. 9A. However, the 2.25Cr-1Mo steel sample tested at 270 MPa shows little signs of microductility and closely resembles the HCM2S sample — Fig. 9C. Figure 10 shows typical cross-sectional LOM photomicrographs acquired from fractured samples of each alloy corresponding to the samples in Fig. 9. The white layer on the fracture edge is an electroless Ni-coating used to preserve the microstructural features near the edge of the sample. Each sample failed intergranularly along prior austenite grain boundaries. Secondary cracks are present behind the fracture surface, with each being approximately normal to the tensile axis. These samples are representative of all energy inputs and PWHT used in this investigation. The cracks in the 2.25Cr-1Mo steel samples tested at 325 MPa (Fig. 10B) appear to have more elongated features as opposed to the relatively undeformed grains seen for the HCM2S in Fig. 10A and the 2.25Cr-1Mo sample tested at 270 MPa — Fig. 10C. This corresponds well with the ductility values presented in Fig. 7.

Discussion

Ductility has been found to be a reliable indicator of stress relief cracking susceptibility when Gleeble simulation techniques are used to compare alloys (Ref. 17). In general, alloys that can appreciably soften during PWHT are capable of relieving residual stresses by macroscopic yielding. On the other hand, alloys that retain their strength at high temperatures and/or become locally embrittled at the grain boundaries are susceptible to low-ductility fracture along the prior austenite grain boundaries during stress relief. Vinckier and Pense (Ref. 18) developed a criteria for the susceptibility to stress-relief cracking of steels based on the percent reduction in area of specimens subjected to HAZ simulations and tested at elevated temperatures (Table 3). The criteria were found to agree with test results by Lundin, *et al.* (Ref. 16), on low-alloy steels.

Table 3 — Steel-Relief Cracking Susceptibility Criteria Developed by Vinckier and Pense (Ref. 18)

Susceptibility to Stress-Relief Cracking	% Reduction in Area
Extremely susceptible	<5%
Highly susceptible	5–10%
Slightly susceptible	10–15%
Not susceptible	>20%

The susceptibility criteria discussed above are to be used as a general guide for well-controlled laboratory experiments. Using these criteria, HCM2S is considered “extremely” to “highly susceptible” to stress-relief cracking at each energy input and postweld heat treatment, whereas, 2.25Cr-1Mo steel would only be considered “slightly susceptible” tested at 325 MPa. The 2.25Cr-1Mo steel samples tested at 270 MPa are considered “slightly” to “highly susceptible” to stress-relief cracking at each PWHT temperature.

The reason for the decrease in ductility of 2.25Cr-1Mo steel when using a lower stress is that a higher stress corresponds to a greater initial strain. In other words, during a constant stress test, the material is initially (prior to the time

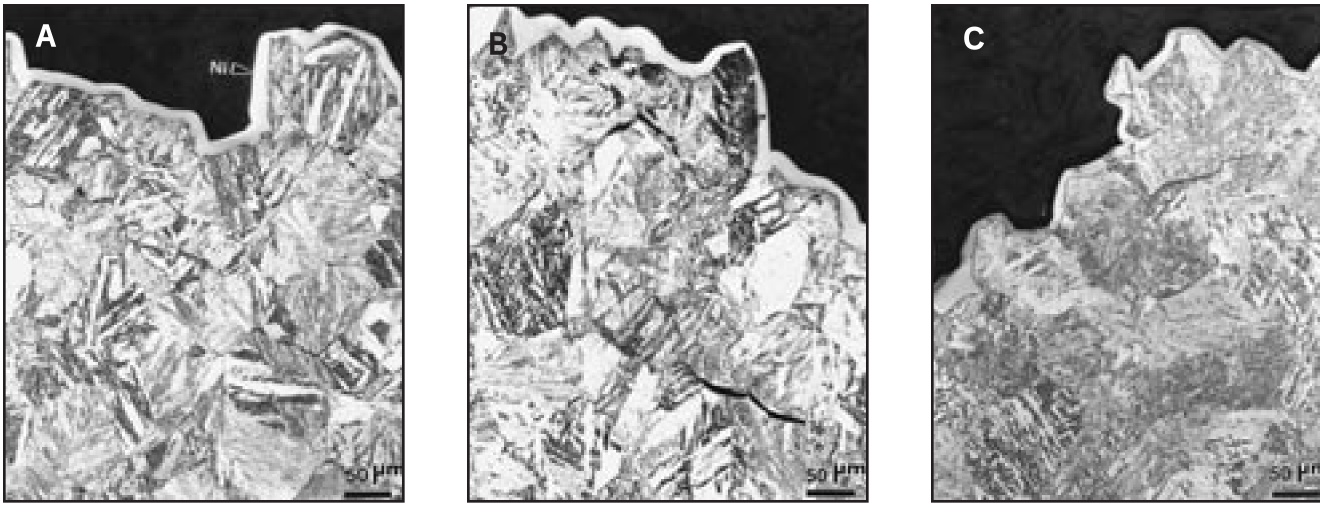

Fig. 10 — Light optical microscopy photomicrographs of cross-sectioned failed samples produced using an energy input of 2 kJ/mm and tested at a PWHT temperature of 675°C. A — HCM2S; B — 2.25Cr-1Mo tested at 325 MPa; C — 2.25Cr-1Mo tested at 270 MPa.

when embrittlement mechanisms are activated) elongated an amount that corresponds to the stress and then the test essentially becomes a creep test. Therefore, the use of a higher stress at a given temperature will initially produce more strain and the apparent ductility increases. Figure 11 is a plot of displacement vs. time for each material/stress test combination at a PWHT temperature of 625°C. The data represents the time at which the PWHT was reached to the time of failure. The increase in stress in the 2.25Cr-1Mo steel has caused an increase in the slope of the steady-state portion of the curve. This is similar to the result of increasing the stress in a creep test. While the elongation initially increases rapidly in each sample, only the 2.25Cr-1Mo steel sample tested at 325 MPa continues to significantly elongate during the remainder of the test. The 2.25Cr-1Mo sample tested at 270 MPa and the HCM2S sample reach a given displacement, then the displacement essentially remains constant. In contrast, the 2.25Cr-1Mo sample tested at 325 MPa continues to elongate and always had a greater rate of elongation than the other samples at all PWHT temperatures. The rate of elongation also increased with increasing PWHT temperature similar to a conventional creep test. Therefore, even though each sample failed due to stress-relief cracking, the 2.25Cr-1Mo samples tested at 325 MPa exhibited high reductions in area and continued to elongate throughout the test. The 2.25Cr-1Mo samples tested at 270 MPa and HCM2S samples experienced some elongation before maintaining a constant displacement and then elongated a small amount before failing due to stress-relief cracking. It is important to note HCM2S should be compared to the 2.25Cr-1Mo samples tested at 270 MPa since, as discussed above, a stress of 325 MPa for 2.25Cr-1Mo steel induces an artificial reduction in area. The lower stress is a more accurate representation of the stress state the 2.25Cr-1Mo steel would experience in an actual weldment because it is closer to the yield strength at the PWHT temperatures used in this study. The result is 2.25Cr-1Mo steel appears to be slightly less susceptible to stress-relief cracking than HCM2S based on the criteria of Vinckier and Pense (Ref. 18). This is especially true since the reduction in area increased as the PWHT temperature increased, but PWHT had no effect on the ductility of HCM2S.

Low ductility intergranular failure in the CGHAZ during PWHT can occur by two general mechanisms: 1) tramp element segregation to prior austenite grain boundaries and/or 2) precipitation strengthening of grain interiors and denuded zone formation near the grain boundaries (Ref. 6). In the former case, the presence of tramp elements (P, S, Sn, As and Sb) along the prior austenite grain boundaries lowers the cohesive strength across the boundaries and leads to brittle, intergranular fracture. In the latter case, alloy carbides (*e.g.* VC, NbC) preferentially precipitate in the prior austenite grain interiors on dislocations and cause considerable strengthening. Along with this, some carbides may precipitate in the prior austenite grain boundaries. These carbides can deplete the adjacent material of carbon leaving a thin precipitate-free denuded zone (Refs. 11, 12). Therefore, any stress will be concentrated in these relatively soft zones leading to intergranular failure. Thus, the operable cracking mechanism of each alloy can be understood by examining the influence of chemical composition on the characteristics of elemental segregation and carbide precipitation and how these processes, in turn, affect the tempering response and fracture modes during stress relief.

Tramp element segregation (temper embrittlement) typically occurs in carbon and low-alloy steels when slowly cooled or isothermally aged in the temperature range of approximately 350–600°C (Ref. 19). When temper embrittled steels are reheated to temperatures above approximately 600°C and cooled rapidly, embrittlement is reversed (Refs. 19, 20). Therefore, with the exception of the samples tested at 575 and 625°C, failure was unlikely to be associated with tramp element segregation.

The CGHAZ of the 2.25Cr-1Mo steel experienced significant softening during postweld heat treatment at 325 MPa whereas the hardness of the CGHAZ of each HCM2S sample after PWHT was essentially identical to the hardness in the as-welded condition. The reason for this difference can be explained by examining the chemical composition and the expected carbide precipitation sequences of these alloys. Baker and Nutting (Ref. 21) studied the carbide precipitation sequence during tempering of 2.25Cr-1Mo steel for a broad range of tempering temperatures (400–750°C) and times (0.5–1000 h). Their findings are illustrated in Fig. 12. The following general carbide precipitation sequence was determined:

$$\varepsilon\text{-carbide} \rightarrow M_3C \rightarrow (Mo_2C + M_3C) \rightarrow M_{23}C_6 \rightarrow M_6C$$

$$(Mo_2C + M_3C) \rightarrow Cr_7C_3 \rightarrow M_6C$$

where the M stands for Fe or Cr.

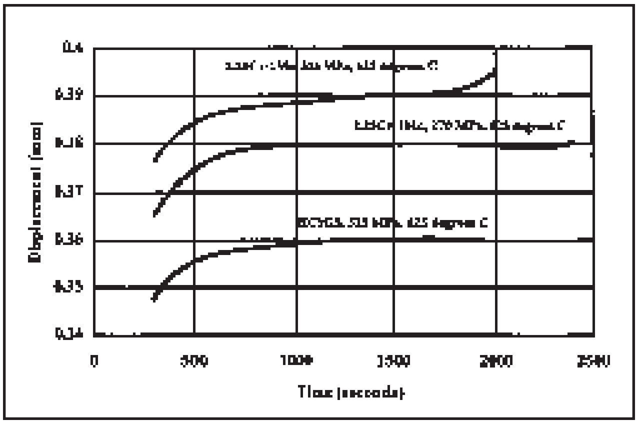

Fig. 11 — Displacement as a function of time during a PWHT of 625°C.

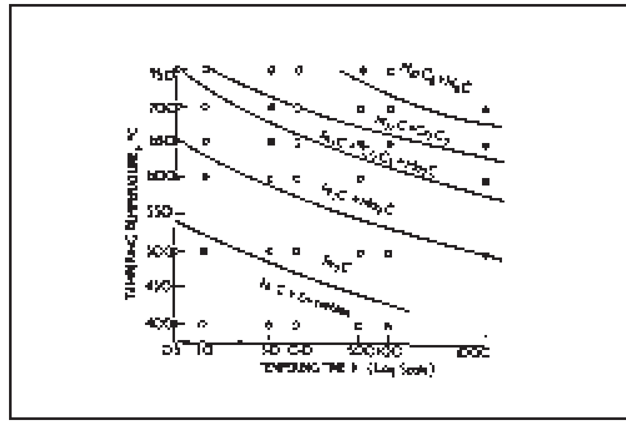

Fig. 12 — Isothermal diagram showing the sequence of carbide formation on tempering of a quenched 2.25Cr-1Mo steel (Ref. 21).

For the temperature range 400–725°C, ε-carbide and/or M_3C always precedes the formation of any Cr- or Mo-based carbides. From these results, it can be estimated that, due to the short times, cementite should be the only carbide to form in the 2.25Cr-1Mo steel samples under the conditions of this study. Therefore, the material should soften relative to the as-welded condition because the mechanism of softening is the release of carbon from the supersaturated matrix and concomitant relaxation of lattice strain (Ref. 22). This would account for the significant increase in ductility observed with increasing PWHT temperature and the low susceptibility to stress relief cracking. This is also consistent with the hardness results in Fig. 8. Because the material could soften appreciably during tempering, the stress would be relieved by macroscopic yielding rather than the concentration of strain at the prior austenite grain boundaries.

The carbide precipitation sequence during the tempering of HCM2S is expected to differ from 2.25Cr-1Mo steel due to the presence of V and Nb, which are strong carbide forming elements. Pigrova (Ref. 23), in a study on quenched and tempered Cr-Mo-V steels, found M_3C (Fe and Cr-rich) and MC (V-rich) carbides to be present after tempering from 450–700°C for up to 1000 h (depending on the temperature). Previous work has shown normalized and tempered HCM2S steel exhibits a fine dispersion of MC along with some M_7C_3 inside the grains and $M_{23}C_6$ along grain boundaries (Ref. 24). The MC carbide was found to be V-rich with some Nb present. After aging for 1000 h at 600°C, MC remained stable, but $M_{23}C_6$ and M_7C_3 transformed to M_6C (Ref. 24). Calculation of phase equilibria at 600°C using Thermo-Calc routine for the C-Cr-1.6W-0.1Mo-0.25V-0.05Nb-0.006N-0.5Mn-0.004B system (Ref. 24) indicated the stable phases at 2.5 wt-%-Cr and 0.06%C are α + VC + M_6C. This is consistent with the long-term aging results. The relatively high susceptibility of HCM2S to stress-relief cracking is likely due to a combination of vanadium carbide precipitation strengthening within the grain interiors and possibly the formation of denuded zones in the grain boundary regions. Denuded zones formed in low-alloy steels are typically only up to a few hundred nanometers wide (Ref. 13). Therefore, even if denuded zones had formed, the detectability is limited to transmission electron microscopy. Vanadium carbide is well-known to promote stress-relief cracking by forming a fine, uniform dispersion of very stable carbides (Refs. 25, 26). Grain interior strengthening by VC would resist stress relaxation by macroscopic yielding and lead to stress intensification along the relatively weak prior austenite grain boundaries that may contain denuded zones. This proposed process would account for the retained hardness of the HCM2S after postweld heat treatment and the relatively high susceptibility to stress relief cracking.

Another possible factor is the presence of B and Al in the HCM2S alloy. Additions of Al (Refs. 13, 27, 28) and B (Refs. 10, 13, 29) to low-alloy steels have been shown to greatly increase the susceptibility to stress-relief cracking and promote the formation of a denuded zone (Ref. 13), although the exact mechanisms by which Al and B promote stress-relief cracking are unclear. Therefore, the differences in composition between 2.25Cr-1Mo steel and HCM2S and their effect on the carbide precipitation kinetics and grain boundary characteristics apparently are the reason for the contrast in the stress-relief cracking behavior. Work is now in progress using analytical and transmission electron microscopy to examine the microstructures so the precise failure mechanisms can be understood in more detail.

Conclusions

The stress relief cracking response of conventional 2.25Cr-1Mo and HCM2S steels was investigated by Gleeble HAZ simulation techniques. The HCM2S alloy was shown to be more susceptible to stress-relief cracking than 2.25Cr-1Mo steel over the range of weld thermal simulations and postweld heat treatment schedules used in this research for single-pass weld CGHAZ simulation samples. HCM2S experienced brittle intergranular failure along prior austenite grain boundaries under each set of test conditions. The 2.25Cr-1Mo steel also failed intergranularly along prior austenite grain boundaries, but exhibited significant macroductility when tested at a stress of 325 MPa. Lowering the applied stress in the 2.25Cr-1Mo steel samples to normalize for the yield strength resulted in lower ductility values from the stress-relief cracking tests. Increasing the postweld heat treatment temperature increased the ductility for 2.25Cr-1Mo steel, but had no significant effect on HCM2S. The as-quenched hardness of the CGHAZ produced at each energy input for 2.25Cr-1Mo steel was ~470 HKN and for HCM2S was ~375 HKN. This difference in as-quenched hardness was attributed to the higher carbon content of the 2.25Cr-1Mo steel. The hardness of the CGHAZ after tempering decreased to ~325 HKN for 2.25Cr-1Mo steel, but remained the same as the as-quenched hardness of the CGHAZ for HCM2S. With the tempering temperatures and times used in this study, ε-carbide and

Fe_3C are expected to precipitate in 2.25Cr-1Mo steel. The concomitant release of carbon from the supersaturated structure and precipitation of Fe_3C results in a decrease in lattice strain and softening of the CGHAZ. In HCM2S, V-rich MC is expected to form, which retards softening and ultimately leads to the higher SRC susceptibility.

Acknowledgments

The authors would like to gratefully acknowledge the sponsors of this research including Sumitomo Metal Corp., Mitsubishi Heavy Industries, Ltd., Foster Wheeler Development Corp. and Pennsylvania Power and Light Co. The authors would also like to thank Dr. Bruce Lindsley for his contributions to this research.

References

1. Masuyama, F., Yokoyama, T., Sawaragi, Y., and Iseda, A. 1994. *Materials for Advanced Power Engineering*. D. Coutsouradis, *et al*. eds., Part 1. Kluwer Academic Publishers, Netherlands, pp. 173–181.
2. Masuyama, F., Yokoyama, T., Sawaragi, Y., and Iseda, A. 1994. *Service Exposure and Reliability Improvement: Nuclear, Fossil, and Petrochemical Plants*, PVP, Vol. 288. ASME, pp.141–146.
3. Prager, M., and Masuyama, F. 1994. *Conference Proceedings Maintenance and Repair Welding in Power Plants V.* Orlando, Fla., EPRI and AWS, pp. 16–30.
4. *Metals Handbook*, 8th ed., Vol. 1. ASM International, Materials Park, Ohio.
5. *Creep Rupture Data of HCM2S Steel Tubes, Pipes, Forgings and Plates*. 1997. Sumitomo Metal Industries, Ltd. and Mitsubishi Heavy Industries, Ltd.
6. Meitzner, C. F. 1975. WRC Bulletin 211 pp. 1–17.
7. Dhooge, A., and Vinckier, A. 1992. *Welding in the World* 30: 44–71.
8. Swift, R. A. 1971. *Welding Journal* 50(5): 195-s to 200-s.
9. Swift, R. A., and Rogers, H. C., *Welding Journal* 50(5): 357-s to 373-s.
10. McPherson, R. 1980. *Metals Forum* 3(3): 175–186.
11. Asbury, F. E., Mitchell, B., and Toft, L. H. 1960. *British Welding Journal* (11): 667–678.
12. Irvine, K. J., Murray, J. D., and Pickering, F. B. 1960. *Journal of the Iron and Steel Institute* (10): 166–179.
13. Edwards, R. H., Barbaro, F. J., and Gunn, K. W. 1982. *Metals Forum* 5(2): 119–129.
14. Nippes, E. F., Merrill, L. L., and Savage, W. F. 1949. *Welding Journal* (28): 556-s to 564-s.
15. Nippes, E. F., and Nelson, E. C. 1958. *Welding Journal* (37): 289-s to 294-s.
16. *Welding Handbook*, 8th ed., Vol. 1. 1991. American Welding Society, Miami, Fla.
17. Lundin, C. D., Liu, P., Qiao, C. Y. P., Zhou, G., Khan, K. K., and Prager, M. 1996. WRC, Bulletin 411, pp. 1–215.
18. Vinckier, A. G., and Pense, A. W. 1974. WRC Bulletin 197.
19. Steven, W., and Balajiva, K. 1959. *Journal of the Iron and Steel Institute* 193: 141–147.
20. Pugh, S. F. 1991. *An Introduction to Grain Boundary Fracture*, The Institute of Metals, London.
21. Baker, R. G. and Nutting, M. A. 1959. *Journal of the Iron and Steel Institute* (7): 257–268.
22. Honeycombe, R. W. K., and Bhadeshia, H. K. D. H. 1996. *Steels: Microstructure and Properties*, 2nd ed. Halstead Press, New York, N.Y.
23. Pigrova, G. D. 1996. *Metallurgical Transactions* A, 27A(2): 498–502.
24. Miyata, K., Igarashi, M., and Sawaragi, Y. 1997. *ICOPE-97*, Tokyo, Japan, pp.13–17.
25. Bentley, K. P. 1964. *British Welding Journal* (10): 507–515.
26. Stone, P. G., and Murray, J. D. 1965. *Journal of the Iron and Steel Institute* (11): 1094–1107.
27. Viswanathan, R., and Beck, C. G. 1975. *Metallurgical and Materials Transactions* A 6A(11): 1997–2003.
28. Ratliff, J. L., and Brown, R. M. 1967. *Transactions of the ASM* 60: 176–186.
29. Presser, R. I., and McPherson, R. 1977. *Scripta Metallurgica* 11: 745–749.

Call for Papers

The 6th International Seminar on Numerical Analysis of Weldability will be held October 1–3, 2001, in Graz, Austria. This seminar is held under the sponsorship of IIW Commission IX, Working Group “Mathematical Modeling of Weld Phenomena.” Papers are invited on the following topics:

- Melt Pool and Arc Phenomena
- Solidification
- Microstructural Modeling in Weld Metal and HAZ
- Microstructure and Mechanical Properties
- Influence of Postweld Heat Treatment
- Crack Phenomena and Testing Methods
- Residual Stresses and Distortion
- Modeling Tools and Computer Programs

Individuals interested in presenting a paper should prepare an abstract no more than a half page in length. Include the title of the paper, name of the author(s) and affiliation. Deadline for abstract submission is April 1, 2001. Send it to Bernhard Schaffernak, TU Graz, Institute for Materials Science, Welding and Forming, Kopernikusgasse 24, A-8010 Graz, Austria; FAX +43 316 873 7187; e-mail bernie@weld.tu-graz.ac.at.